Hindawi
Shock and Vibration
Volume 2018, Article ID 3463528, 13 pages
https://doi.org/10.1155/2018/3463528

Research Article

Vibration Suppression of a Cantilever Plate Using Magnetically Multimode Tuned Mass Dampers

Jae-Sung Bae, Jung-Sun Park, Jai-Hyuk Hwang, Jin-Ho Roh, Bong-do Pyeon, and Jong-Hyuk Kim

School of Aerospace and Mechanical Engineering, Korea Aerospace University, 200-1 Hwajeon-dong, Deogyang-gu, Goyang-si, Gyeonggi-do 412-791, Republic of Korea

Correspondence should be addressed to Jae-Sung Bae; jsbae@kau.ac.kr

Received 15 July 2017; Accepted 20 February 2018; Published 12 April 2018

Academic Editor: Abdul Qadir Bhatti

Copyright © 2018 Jae-Sung Bae et al. This is an open access article distributed under the Creative Commons Attribution License, which permits unrestricted use, distribution, and reproduction in any medium, provided the original work is properly cited.

For a few decades, various methods of suppressing structural vibration have been proposed. The present study proposes and exploits an effective method of suppressing the vibration of cantilever plates similar to the solar panels of a satellite. Magnetically tuned mass dampers (mTMDs) are a tuned mass damper (TMD) with eddy current damping (ECD). We introduce the mTMD concept for the multimode vibration suppression of the cantilever plate. The design parameters of the mTMD are determined based on the parametric study of the theoretical four-degree-of-freedom model, which was derived for a cantilever plate with TMDs. Two TMDs are optimized for the first bending mode and first torsion mode of the plate, and they are verified analytically and experimentally. To increase the damping performance of the TMDs, ECD is introduced. Its damping ratios are estimated analytically and verified experimentally.

1. Introduction

The suppression of structural vibrations has significant applications in engineering fields such as machine tool industries, as well as with civil, automotive, and aerospace structures. Over the past few decades, significant research effort has been applied to suppressing vibrations in engineering structures and machines. Traditionally, passive methods have been used to attenuate structural vibrations. Recent advances in digital signal processing and sensor/actuator technology have resulted in a substantial focus on using active methods [1]. In addition, semiactive methods have filled the gap between the two.

Eddy currents are generated when a conducting plate moves in the stationary magnetic field or the magnetic field varies on the stationary conducting plate. The relative motion between the conducting plate and the magnetic field induces the eddy currents within the conducting plate. These currents induce their own magnetic field with the opposite polarity of the applied magnetic field so that the resistive electromagnetic force is generated. This electromagnetic force eventually disappears due to the electrical resistance and is proportional to the velocity of oscillating conductor. Hence the ECD can be allowed to function as a form of viscous damping.

A lot of studies on various applications utilizing eddy currents for damping dynamic systems have been developed in past decades [2–8]. Sodano and Bae [9] and Bae et al. [10, 11] have already presented a good literature review. Kwak et al. [12] introduced an eddy current damper (ECD) and applied it to the vibration suppression of a cantilever beam. Their experiments showed that an ECD was very effective for the vibration suppression of a cantilever beam. Bae et al. [13] developed a mathematical model for the ECD of Kwak et al. [12]. Using this model, they have investigated the ECD damping characteristics and performed the simulation of the vibration suppression of a cantilever beam with Kwak's ECD. Sodano et al. [14–16] proposed the new concept of ECD device to attenuate the vibration of a cantilevered beam. Cheng and Oh [17, 18] studied multimode vibration suppression using a permanent magnet and a coil with a shunt circuit for semiactive control.

Recently, Bae et al. [10] proposed using a magnetically tuned mass damper (mTMD), as shown in Figure 1, to increase the damping performance of a conventional TMD

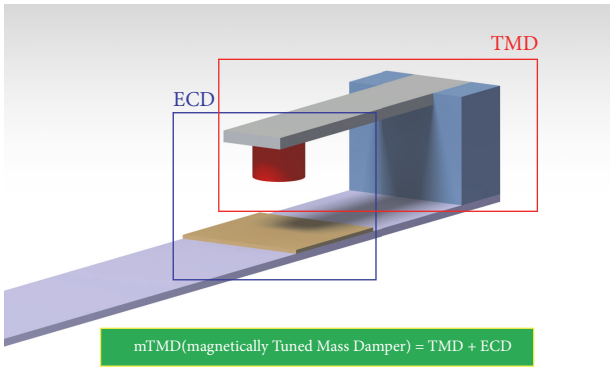

Figure 1: Schematic of magnetically tuned mass damper [10].

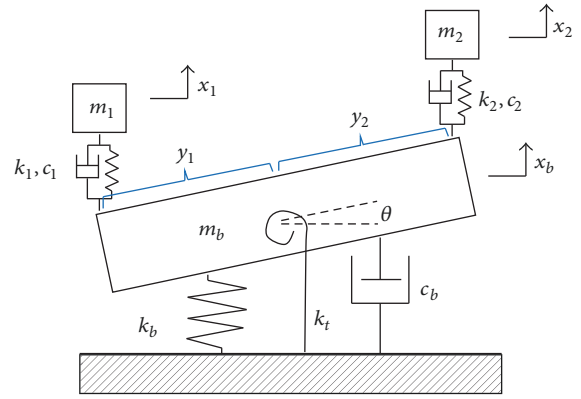

Figure 2: Schematic of a multimode TMD (4-DOF).

by using eddy current damping (ECD). Their study used simulations and experiments to show that the proposed method significantly increased the damping performance of the TMD if not adequately tuned. Wang et al. [19] derived the theoretical formulation of ECD in a horizontal TMD. They constructed a large-scale horizontal TMD with ECD and investigated its characteristics experimentally. Yan et al. [20] proposed and studied the multimode vibration suppression method employing a permanent magnet stacked electromagnetic absorber with negative resistance and negative inductance negative resistance shunt impedances. They showed numerically that the proposed absorber could absorb the multimode vibration of a beam and provide considerable damping over a relatively wider bandwidth. Yan et al. [21] proposed an electromagnetic shunt damping vibration isolator consisting of a box-shaped spring, a permanent magnet, an electromagnet, and a shunt circuit. Their numerical results showed that the proposed isolator could attenuate the vibration of a plate considerably. Xie et al. [22] proposed and developed an electromagnetic shunt damping absorber (EMSDA) employing an electromagnetic shunt damping mechanism. They derived the theoretical model of the EMSDA and showed numerically and experimentally that the proposed absorber could suppress the structural vibration significantly. Zihao et al. [23] proposed a beam-like semiactive electromagnetic vibration absorber (EVA) consisting of a flexible ferromagnetic cantilever beam, a ferromagnetic mass, and an E-shaped electromagnet. Their numerical and experimental results showed that the proposed EVA effectively suppressed vibrations under both steady-state excitation and sweeping frequency excitation. Bae et al. [24] proposed a relatively lightweight TMD to attenuate the vibration of a large beam structure by introducing eddy current damping to a TMD. This method was an application of their previous work [10]. The experimental results showed that the proposed method was simple but effective in suppressing the vibration of a large beam structure without a substantial weight increase.

The lowest two modes of a cantilever plate are generally the first bending mode and the first torsion mode. Both modes could be important in the vibration suppression of the plate. The present study introduces the mTMD concept for the multimode vibration suppression of a plate. The four-degree-of-freedom model of a cantilever plate with TMDs is employed for a theoretical analysis. Two TMDs are optimized for the first bending mode and first torsion mode of the plate, and they are verified analytically and experimentally. ECD is introduced to increase the damping performance of the TMDs. Its damping ratios are estimated analytically and verified experimentally.

2. Theoretical Analysis

2.1. Theoretical Modeling of a Multimode TMD. The schematic of a multimode TMD with damping in both the base and adaptive mass system is shown in Figure 2. From this schematic, the relative displacement between the base and each adaptive mass (m_1 and m_2) is calculated using (1). The rotational angle (θ) of the base is assumed to be small.

$$\begin{aligned} &x_1 - x_b + y_1\theta : \text{ between the base and } m_1 \\ &x_2 - x_b - y_2\theta : \text{ between the base and m}_2. \end{aligned} \tag{1}$$

To obtain the equations of motion from Lagrange's equation, the kinetic energy and the potential energy of the system can be written as

$$\begin{aligned} T &= \frac{1}{2}m_b\dot{x}_b^2 + \frac{1}{2}\left(J_b + m_1y_1^2 + m_2y_2^2\right)\dot{\theta}^2 + \frac{1}{2}m_1\dot{x}_1^2 \\ &\quad + \frac{1}{2}m_2\dot{x}_2^2 \\ V &= \frac{1}{2}k_bx_b^2 + \frac{1}{2}k_t\theta^2 + \frac{1}{2}k_1\left(x_1 - x_b + y_1\theta\right)^2 \\ &\quad + \frac{1}{2}k_2\left(x_2 - x_b - y_2\theta\right)^2. \end{aligned} \tag{2}$$

The generalized force can be defined as

$$\begin{aligned} F &= \frac{1}{2}c_b\dot{x}_b^2 + \frac{1}{2}c_t\dot{\theta}^2 + \frac{1}{2}c_1\left(\dot{x}_1 - \dot{x}_b + y_1\dot{\theta}\right)^2 \\ &\quad + \frac{1}{2}c_2\left(\dot{x}_2 - \dot{x}_b - y_2\dot{\theta}\right)^2. \end{aligned} \tag{3}$$

Table 1: Plate properties.

Length	Width	Thickness	Young's modulus	ν	ρ
280 mm	290 mm	2 mm	72 GPa	0.32	2630 kg/m^3

From the Lagrange's equation, the equations of motion are presented as

$$\begin{bmatrix} m_b & 0 & 0 & 0 \\ 0 & J_b + m_1 y_1^2 + m_2 y_2^2 & 0 & 0 \\ 0 & 0 & m_1 & 0 \\ 0 & 0 & 0 & m_2 \end{bmatrix} \begin{Bmatrix} \ddot{x}_b \\ \ddot{\theta}_b \\ \ddot{x}_1 \\ \ddot{x}_2 \end{Bmatrix} + \begin{bmatrix} c_b + c_1 + c_2 & -c_1 y_1 + c_2 y_2 & -c_1 & -c_2 \\ -c_1 y_1 + c_2 y_2 & c_t + c_1 y_1^2 + c_2 y_2^2 & c_1 y_1 & -c_2 y_2 \\ -c_1 & c_1 y_1 & c_1 & 0 \\ -c_2 & -c_2 y_2 & 0 & c_2 \end{bmatrix} \begin{Bmatrix} \dot{x}_b \\ \dot{\theta}_b \\ \dot{x}_1 \\ \dot{x}_2 \end{Bmatrix} + \begin{bmatrix} k_b + k_1 + k_2 & -k_1 y_1 + k_2 y_2 & -k_1 & -k_2 \\ -k_1 y_1 + k_2 y_2 & k_t + k_1 y_1^2 + k_2 y_2^2 & k_1 y_1 & -k_2 y_2 \\ -k_1 & k_1 y_1 & k_1 & 0 \\ -k_2 & -k_2 y_2 & 0 & k_2 \end{bmatrix} \begin{Bmatrix} x_b \\ \theta_b \\ x_1 \\ x_2 \end{Bmatrix} = \begin{bmatrix} F \\ 0 \\ 0 \\ 0 \end{bmatrix} \sin \omega t. \quad (4)$$

To verify the equation of motion, a comparison with the results of a commercial FEM program is carried out. The analysis is performed according to the mass ratio of the plate and TMD. Figure 3 shows the frequency results of the modeling and program, and it indicates that the two models are in good agreement with the error at 1%. Table 1 presents the properties and specifications used in the analysis.

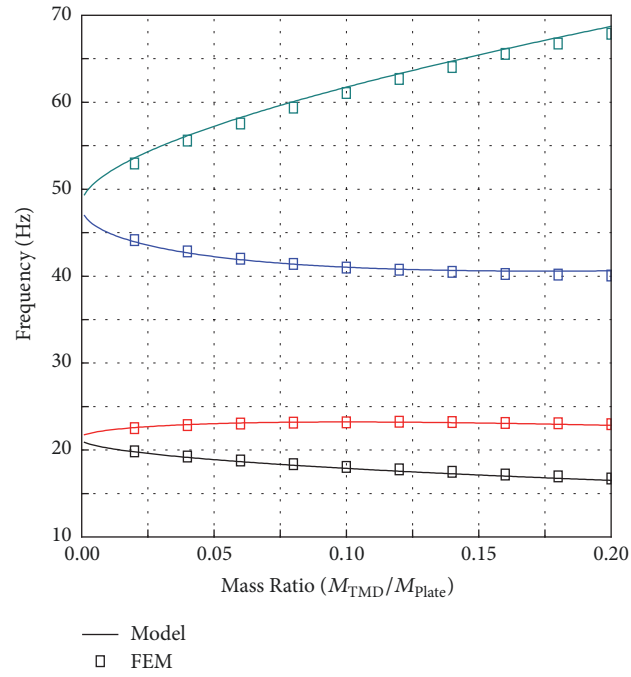

Figure 3: Comparison of frequency results for the presented modeling and commercial FEM program for various mass ratios.

2.2. Modeling of Eddy Current Damping. A few concepts of the ECD devices are proposed by researchers in decades. The concept of the ECD used in the present study is presented in Figure 4 and is proposed by Sodano et al. [14–16] and Bae et al. [10]. The damping force (F_z) in the z (vertical) direction due to the eddy current in Figure 4 yields

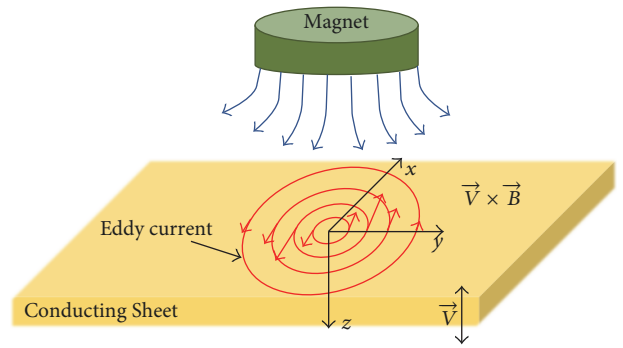

Figure 4: Schematic of eddy currents [10].

$$F_z = -2\pi\sigma\delta\nu \int_0^{r_c} y {B_y}^2 \left(y, l_g\right) \mathrm{d}y = -2\pi\sigma\delta\nu \left(\frac{\mu_0 M_0 b}{4\pi}\right)^2 \cdot \int_0^{r_c} \int_{-L}^{0} y \left(l_g - z_1\right) {I_1}^2 \left(b, y, l_g - z_1\right) \mathrm{d}z_1 \mathrm{d}y, \quad (5)$$

where the details of (5) are referred to [10].

2.3. Cantilever Plate with Magnetically Tuned Mass Dampers. Figure 5 shows a TMD with ECD applied to a cantilever plate. This TMD with ECD is called a magnetically tuned mass damper (mTMD). The mTMD consists of a permanent magnet, a cantilevered beam, and a conducing plate of sheet. Two mTMDs are implemented via the attachment of an additive structure on both sides of the cantilever plate. One is used to suppress the first bending vibration, and the other is used to suppress the first torsional vibration. In terms of performance, TMDs offer excellent vibration absorption in a particular frequency range, but they are unsatisfactory outside of that range. In the present study, ECD is used to improve the performance of a TMD in a wide frequency range. In the present study, TMDs are first

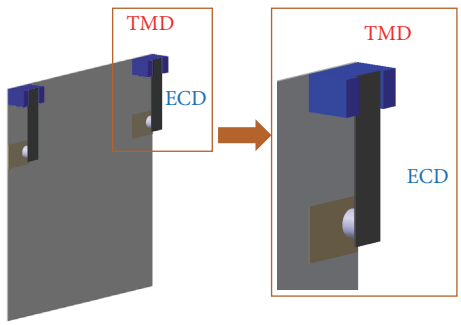

Figure 5: Schematic of magnetically tuned mass damper.

designed to suppress the vibrations of a cantilevered plate, and the vibration absorption performance is verified via experiments and simulations. ECD is subsequently applied to the TMDs to improve their performance, and the mTMDs are verified via experiments.

3. Numerical and Experimental Results

3.1. TMD Design Parameters. Generally, as the mass ratio μ of the TMD mass to the primary mass increases, the damping performance of a TMD on the vibration of the primary structure becomes more effective. However, it causes the mass increase of the system. Therefore, it is necessary to limit the value of μ. Since the value of μ is practically assumed to be from 0.05 to 0.25 the largest value must be selected to improve TMD performance.

When $\mu = 0.25$ and $\zeta = 0.01$, the normalized magnitude of the primary structure for various β and ζ values is presented in Figure 6. In Figure 6(a), the TMD shows good vibration absorption performance at $\beta = 0.85$, so this value is selected. Figure 6(b) shows the normalized magnitude of the primary structure for various ζ values, and it is known that an optimized damping ratio exists at which the performance of the vibration absorption reaches its maximum value.

However, the optimal parameters of the TMD change when multimode TMDs are employed. To determine the effects of absorber frequency, the mass ratios of two TMDs are fixed at 0.1. Figure 7(a) shows the tendency according to frequency ratio. As the frequency ratio increases, the amplitude peak of the primary structure increases. Also, Figure 7(b) shows that the frequency ratio is fixed at 0.9 for the parameter study. Changing the mass ratio causes the gap between peaks to increase.

When the mass ratio is 0.1, the frequency ratio of the TMD in terms of suppressing the bending vibration is 0.96. Figure 8(a) shows the frequency response for this case. The TMD tuned for the bending mode affects the peak of the bending vibration, but the torsion vibration only changes the frequency of the peak; it does not diminish the amplitude. Figure 8(b) shows the frequency response when the frequency ratio for the torsion is 0.95.

Using optimal parameters for each TMD, the suppression performance tends not to be optimized due to the coupling effect. That is why additional tuning is required. Considering that the bending and torsion vibrations are suppressed optimally, the TMD frequency ratios are tuned at $\beta_1 = 0.91$ and $\beta_2 = 0.92$. Figures 9(a) and 9(b) show the frequency responses when TMDs are tuned individually and simultaneously, respectively. The damping performance of TMDs tuned for both bending and torsion is more excellent as shown Figure 9(b).

3.2. TMD Experimental Setup and Results

3.2.1. Theoretical and Experimental Results. First, mathematical modeling was verified in Section 2 before the TMD experiment. Figure 10 shows the experimental results for the frequency response function for the theoretical modeling of the plate. The boundary conditions of the two results are that the bottom of the plate is fixed and TMD (absorber) system is not installed.

The first and second natural frequencies obtained in theoretical modeling are 19.91 Hz and 44.95 Hz. And the mode natural frequencies obtained by the experiment are 19.96 Hz and 45.02 Hz, respectively. Since the error of each mode frequency is about 0.25%, 0.16%, which is less than 1%, the validity of mathematical modeling has been verified.

3.2.2. TMD Experimental Setup and Results. Figure 11 shows the experimental setup with the TMDs attached to a plate. Acrylic connectors are used to construct the TMDs, and the mass is 5.8 g. For convenience, the plate is designated as the primary structure, the TMD tuned for bending vibrations is called the first TMD, and the TMD tuned for torsional vibrations is called the second TMD. The experiments are carried out on the basis of the design parameter $\mu = 0.1$, and they are performed using a laser displacement sensor and impact hammer.

The experiments are performed according to a series of procedures. To compare the results, the first vibration test is conducted only on the primary structure. In order to reduce the vibration for the bending mode, the first TMD is applied to the primary structure and the second TMD is applied to reduce the vibration for the torsional mode. Figure 12 shows the FRF results. The FRF of the primary structure is denoted using a black line for comparison with other results. In the first mode, which is the bending mode, the frequency is about 19.91 Hz. In the second mode, the torsion mode, the frequency is about 44.86 Hz. When only the first TMD is attached, the bending vibration is effectively attenuated at about 16.2 dB, but the torsional vibration is not suppressed. When only the second TMD is attached, similarly, only the torsional vibration is suppressed at about 16.19 dB. From these results, the vibration absorption performance of the TMDs is verified as being suitable for each mode. However, when the TMD is only applied for a single mode, the other mode is not affected.

In order to suppress the bending and torsion vibrations together, the first and second TMDs are applied simultaneously. Each TMD is seated on the basis of the design parameter of the optimized single mode. Figure 13 shows the FRF results. The FRF results in Figure 13(a) show that the

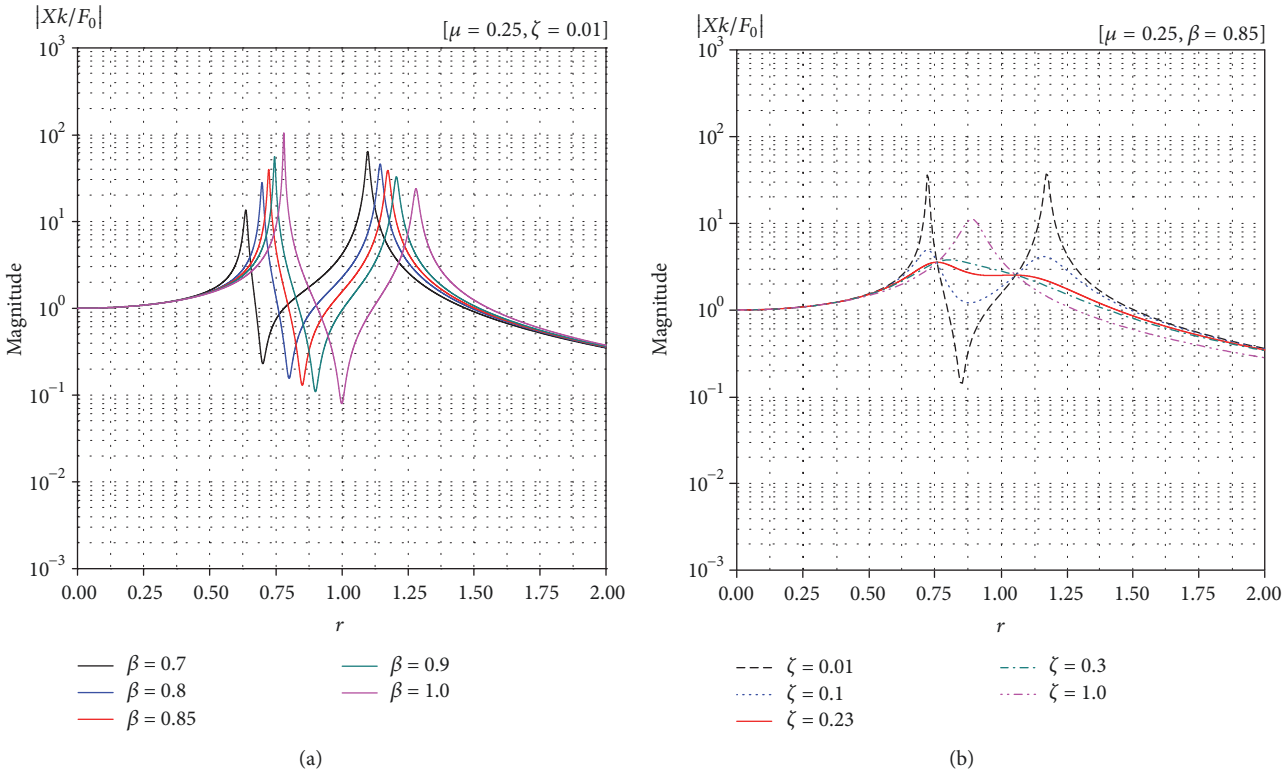

FIGURE 6: Normalized magnitude of the primary structure: (a) for various β values when $\mu = 0.25$; (b) for various ζ values when $\mu = 0.25$, $\beta = 0.85$.

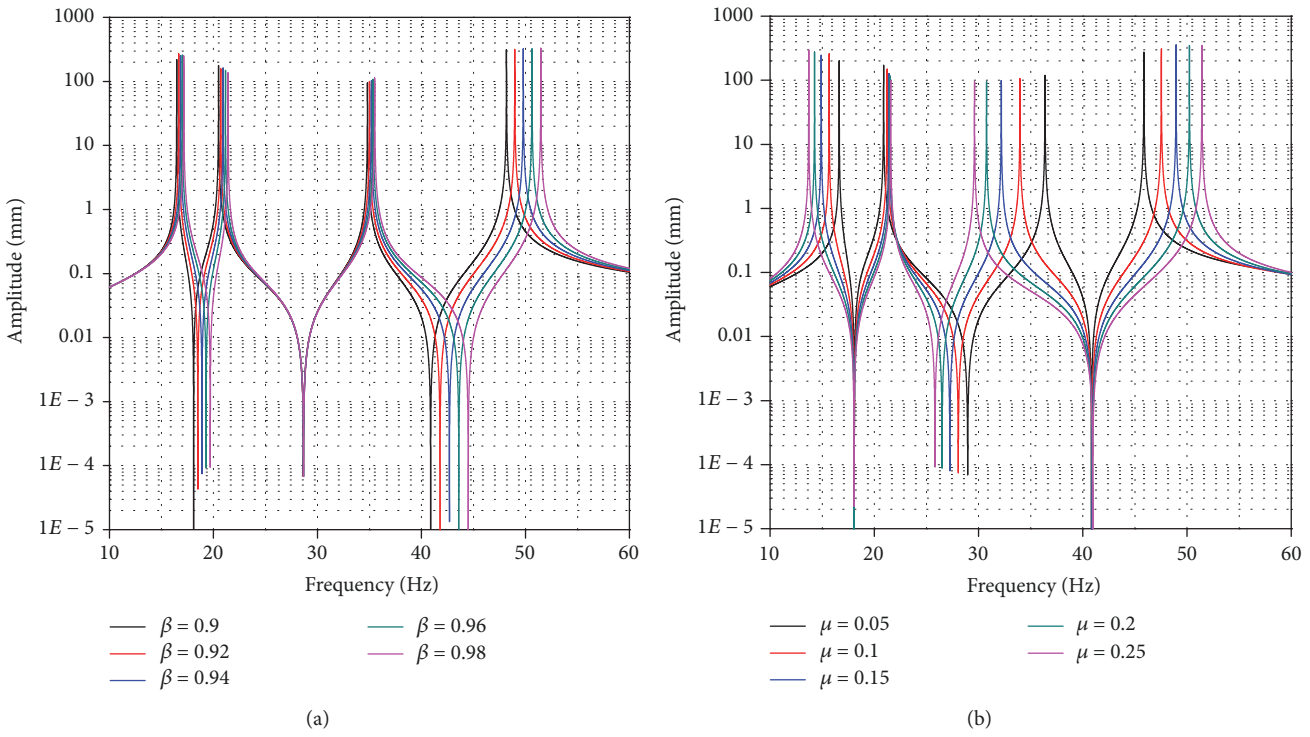

FIGURE 7: Normalized magnitude of the primary structure: (a) for various β values when $\mu = 0.1$ and (b) for various μ values when $\beta = 0.9$.

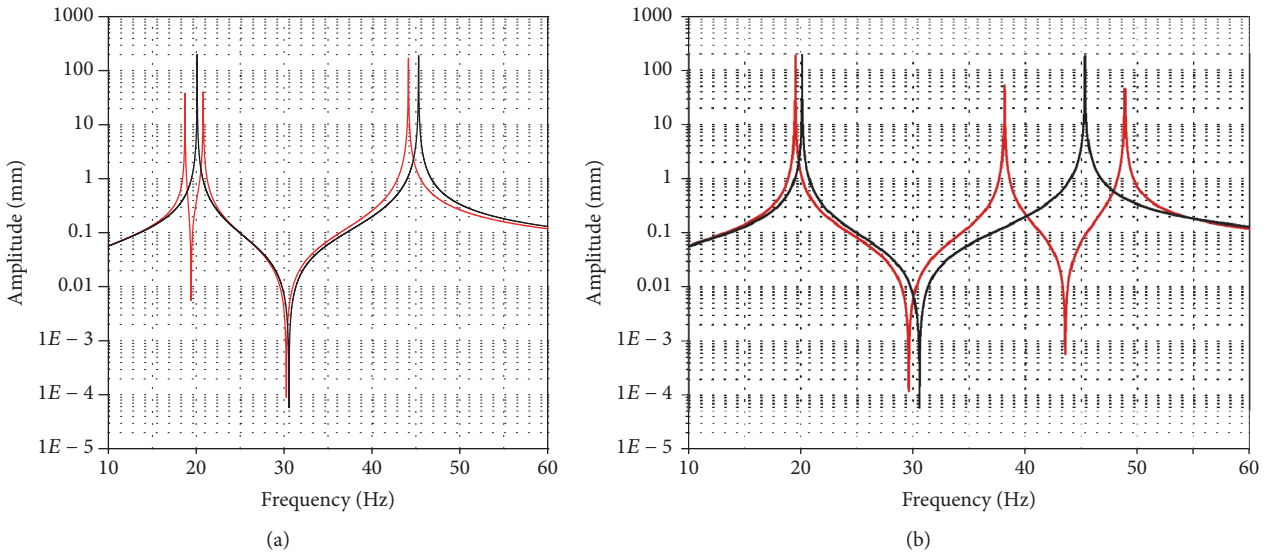

FIGURE 8: Normalized magnitude of the primary structure: (a) with the bending TMD and (b) with the torsion TMD (Key: black line, Primary: red line, TMD.).

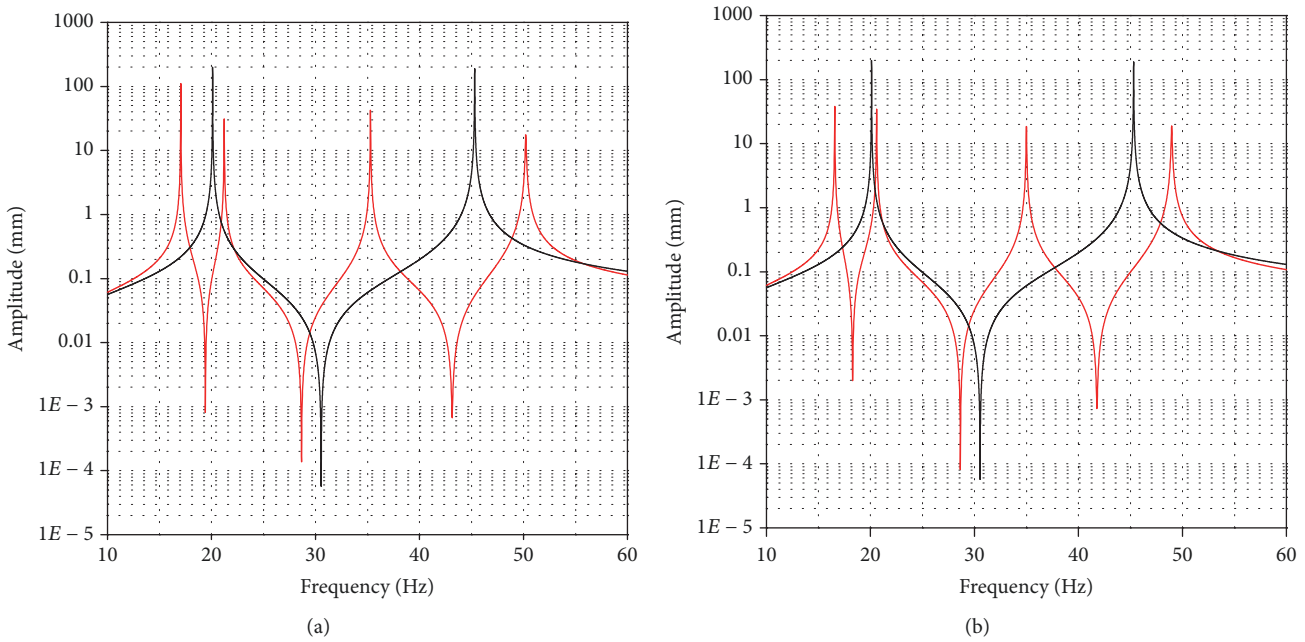

FIGURE 9: Frequency response functions of the plate with the TMDs: (a) with the TMDs tuned individually and (b) with the TMDs tuned for both bending and torsion (Key: black line, Primary: red line, TMD.).

TMDs are not optimized because the coupling effect does not correspond with the peak values. Therefore, it can be seen that a new optimal design parameter is needed.

Using a new optimal parameter that considers the coupling effect, vibration tests are carried out repeatedly. The results are shown in Figure 13(b). The bending vibration suppresses about 9.75 dB to 10.52 dB, and the torsional vibrations are attenuated at about 14.05 dB to 14.15 dB. Each TMDs is optimized and suppresses the vibrations effectively.

3.3. Experimental Results and Simulations of Magnetically TMD. Figure 14 shows the experimental setup of the mTMD using magnetic effects to improve the vibration absorption performance of the TMD. The conducting sheet is located in the magnetic field generated by a cylindrical permanent magnet used as a concentrated TMD mass.

The eddy currents circulate on the conducting sheet via the relative motion between the magnet and the conducting sheet. In addition, ECD can be generated. The thickness of

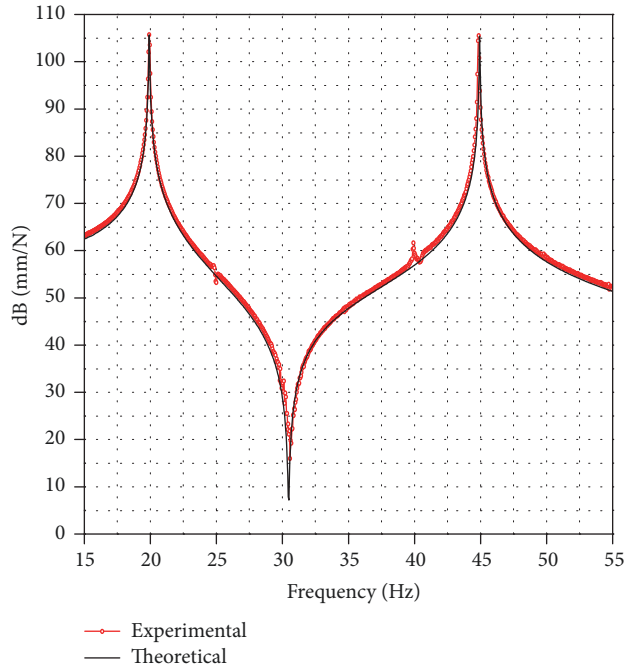

Figure 10: Comparison of theoretical and experimental results for only plate.

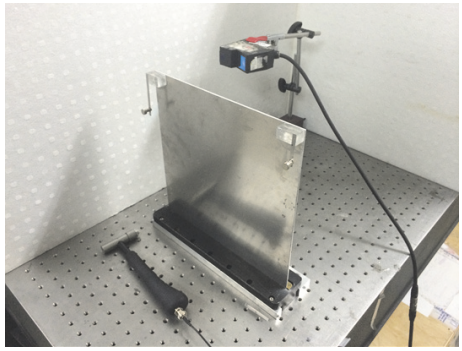

Figure 11: TMD experimental setup.

the conducting sheet is 0.4 mm. The gap between the magnet and conductive sheet can be changed by using externally fixed blocks. Figure 15 shows the experimental results when the gap between the first TMD magnet and the conductive sheet is 3 mm and the second TMD's gap is 1 mm. From these results, it is known that the performance of the present mTMD surpasses that of the TMD. The mTMD shows excellent damping effects in a wide frequency range.

3.4. Effects of Gap on Magnetically TMD Performance. As shown in Figure 16, the theoretical results of the mTMD show how the gap between the magnet and the conductive sheet affects the performance of the vibration absorption of the mTMD. The gap size is reduced from 5 mm to 1 mm by moving fixed blocks between the magnet and the beam of the TMD during the experiments. To verify the damping effect according to the gap, first, the gap of the first TMD is fixed. The experiments are then performed for various gaps of the second TMD. The experiments are subsequently repeated with the same procedure after changing the gap of the first TMD. Figure 16 shows the FRF results for in each case. However, as shown in Figure 7, TMD performance is not proportional to the damping ratio (ζ), and the optimal value of the damping ratio is about 0.23. The optimal value of the gap size in the present mTMD system is 3 mm as shown in Figure 17 and Table 2 (the theoretical approach used to calculate the damping ratio of the mTMD will be presented in the next section.) Table 2 shows the degree of attenuation in dB of each order of natural frequency. Each datum in Table 2 represents the maximum reduction width. The 3 mm gap is chosen because it has the largest energy in the first bending mode, so the gap of the first TMD with the maximum reduction width is set at 3 mm. In addition, the gap of the second TMD shows a gradual decrease in the vibration reduction width when the first TMD gap is increased by 3 mm. Based on these results, it can be known that the gap of the TMDs optimized for vibration suppression performance are 3 mm and 1 mm, respectively.

3.5. Theoretical Analysis of mTMD Damping Coefficient. Previous experiments confirm that the damping ratio of an mTMD can be controlled by changing the gap between the magnet and conductive sheet. These damping characteristics can be explained by (5).

Equation (5) calculates the amount of ECD force generated during the relative motion between the magnet and conductor, so the magnetic damping coefficient can be obtained by eliminating the term of velocity (v) in the equation. Regarding the various gap sizes from 1 to 5 mm,

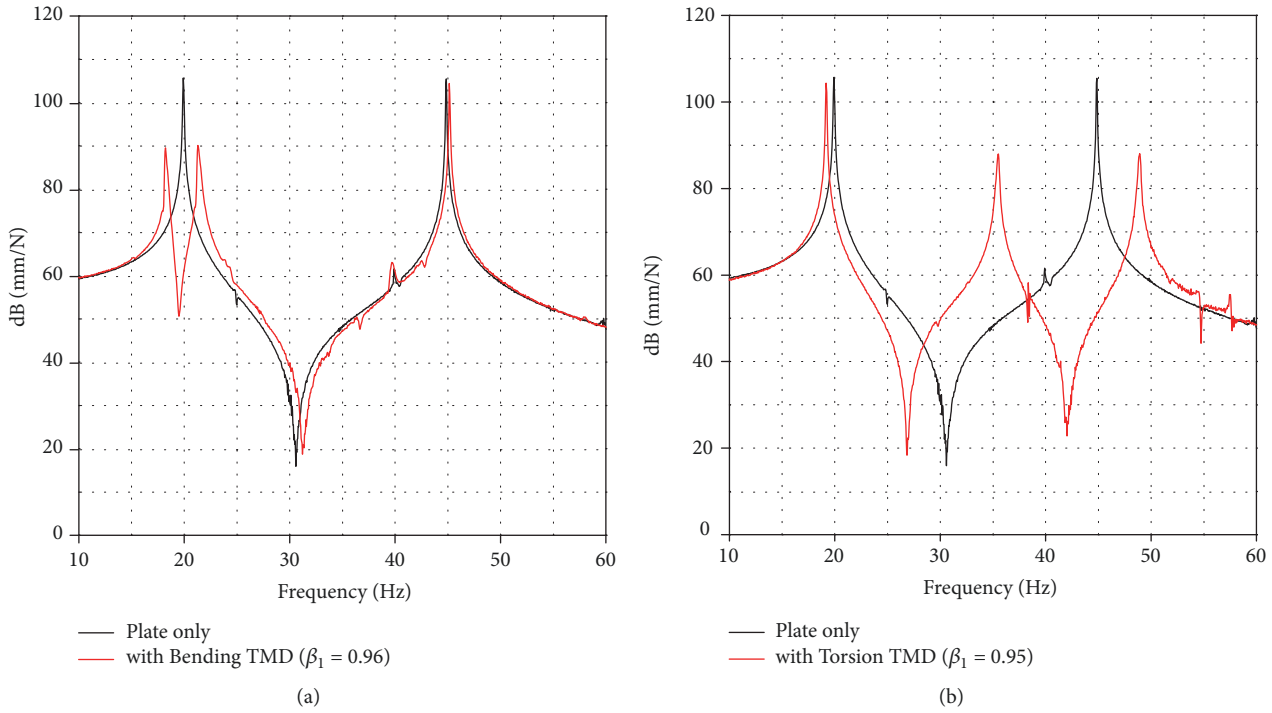

Figure 12: Experimental FRF results of the primary structure with each TMD: (a) with the first TMD only and (b) with the second TMD only (Key: black line, Primary: red line, TMD).

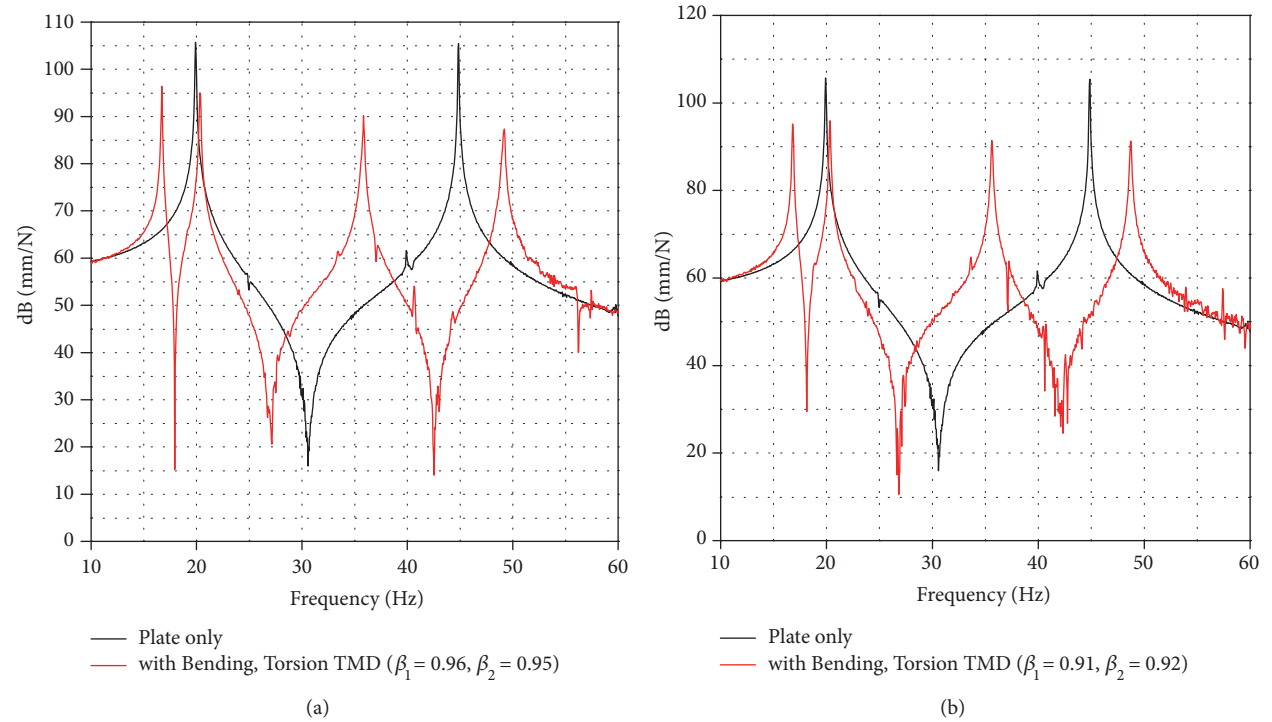

Figure 13: Experimental FRF results of the primary structure with TMDs: (a) with the TMDs tuned individually and (b) with the optimized TMDs (Key: black line, Primary: red line, TMD).

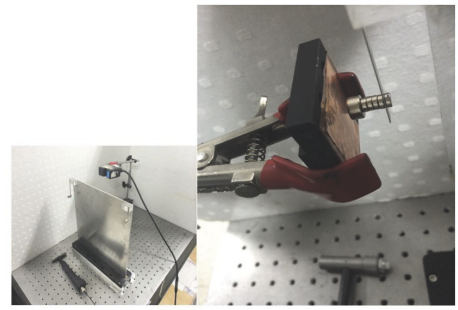

Figure 14: Experimental setup of the mTMD.

Table 2: Experimental results of the mTMD with respect to gap interval [Unit: dB].

Gap of second TMD	Gap of first TMD				
	1 mm	2 mm	3 mm	4 mm	5 mm
1 mm	−31.59/−35.97	−32.96/−37.21	−37.21/−36.48	−33.99/−36.45	−33.67/−36.69
2 mm	−30.41/−34.42	−31.22/−34.19	−34.19/−34.17	−32.82/−34.62	−32.01/−33.71
3 mm	−28.98/−32.12	−30.41/−32.13	−32.13/−32.22	−31.32/−31.23	−30.35/−30.83
4 mm	−28.13/−30.08	−29.65/−29.62	−30.63/−29.85	−30.58/−29.51	−29.09/−28.86
5 mm	−27.52/−27.64	−28.89/−28.16	−30.05/−27.58	−29.94/−27.02	−28.31/−25.883

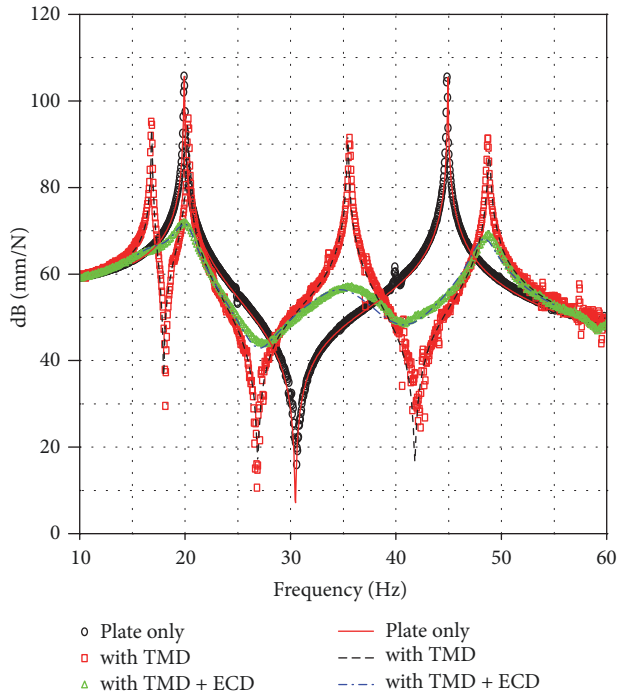

Figure 15: Experimental FRF results of the primary structure with the mTMD.

the magnetic coefficients calculated using (5) are presented in Table 3. These results theoretically verify the fact that the decrease in the gap causes the magnetic damping coefficient to increase. This can be proven with experiments using only the mTMD. Table 3 compares the damping ratio between the experiments and theoretical analyses.

For the first TMD, the optimal value of the gap size in the simulation results (3 mm) is identical to the value in the experimental results. Figure 17 shows the damping ratio of the first mode for various gap sizes. The simulation and experimental results are in good agreement. From the results described above, the present method of calculating the magnetic damping coefficients can be verified.

4. Conclusions

The present study proposed the mTMD concept to suppress the multimode vibration of a cantilevered plate. The four-degree-of-freedom model is employed to theoretically describe the vibration of a cantilevered plate with TMDs. Two TMDs are optimized for the first bending mode and first torsion mode of the plate, and they are verified analytically and experimentally. ECD is introduced to increase the damping performance of the TMDs. The damping model of ECD in [10] is used to calculate the damping force of mTMD. Its damping ratios are estimated analytically and verified experimentally.

For the multimode vibration suppression, two mTMDs are introduced to the cantilevered plate. The damping performance of the plate with two mTMD is estimated analytically. To verify the analytical results, the experimental setup is constructed. The results show that the mTMDs to be optimized for both the bending and torsion modes could attenuate the multimode vibration of the plate efficiently in a wide frequency range. The gap size between the magnet and the conductor is one of important parameters to determine the damping ratio of ECD. The present estimations of the damping ratios for various gap sizes are in good agreement with the experimental results.

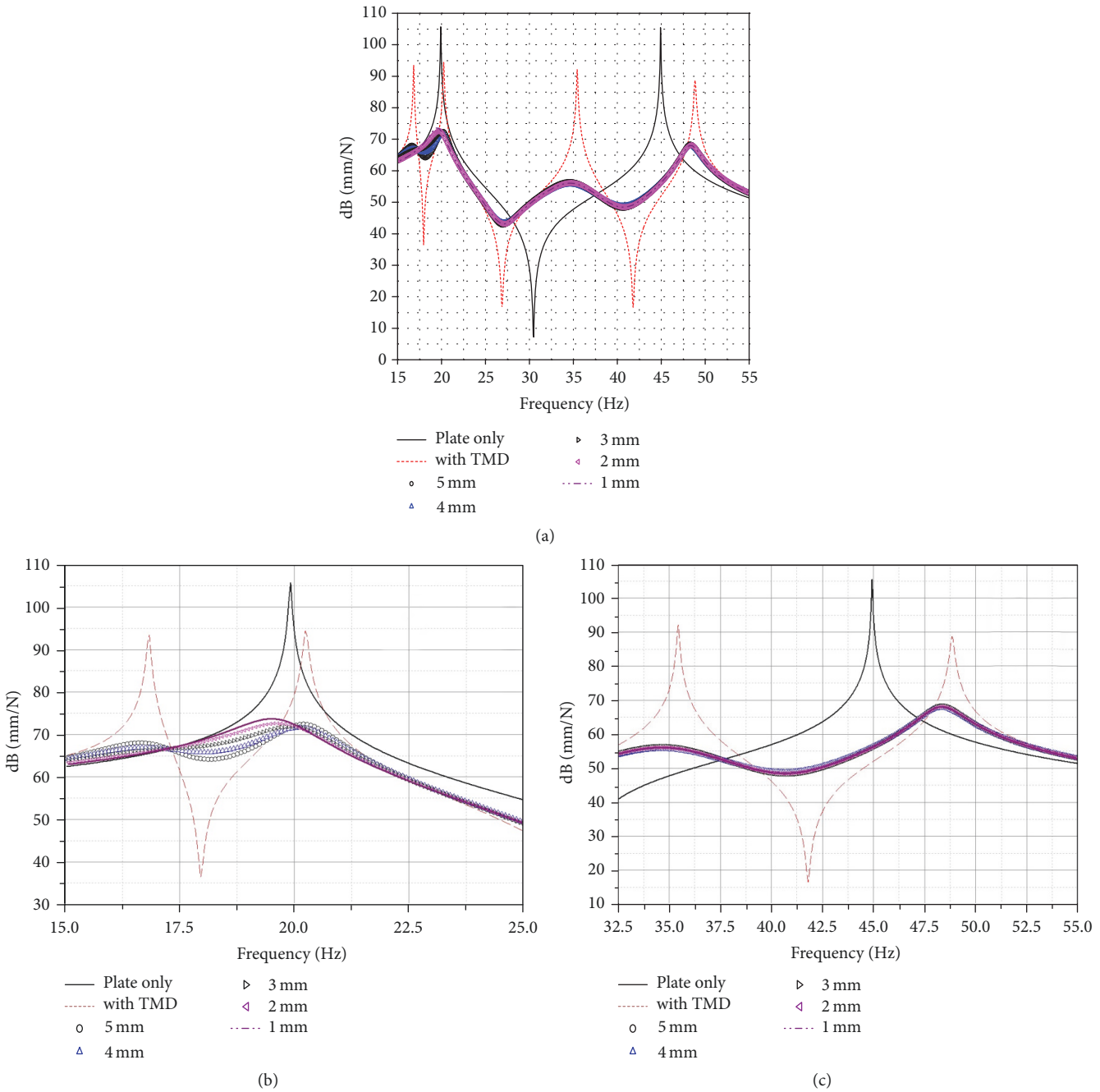

Figure 16: Effect of the gap size of the primary structure: (a) with the mTMD, (b) with the mTMD in bending mode, and (c) with the mTMD in torsion mode.

Table 3: Comparison of damping coefficients for the gap change between experiments and theoretical analyses.

Gap	Bending		Torsion	
	Experiment	Theoretical analysis	Experiment	Theoretical analysis
5 mm	0.08151	0.0739	0.0299	0.0289
4 mm	0.09727	0.0998	0.0372	0.0365
3 mm	0.1347	0.1388	0.0512	0.0480
2 mm	0.2094	0.2009	0.0644	0.0663
1 mm	0.2730	0.2702	0.0850	0.0868

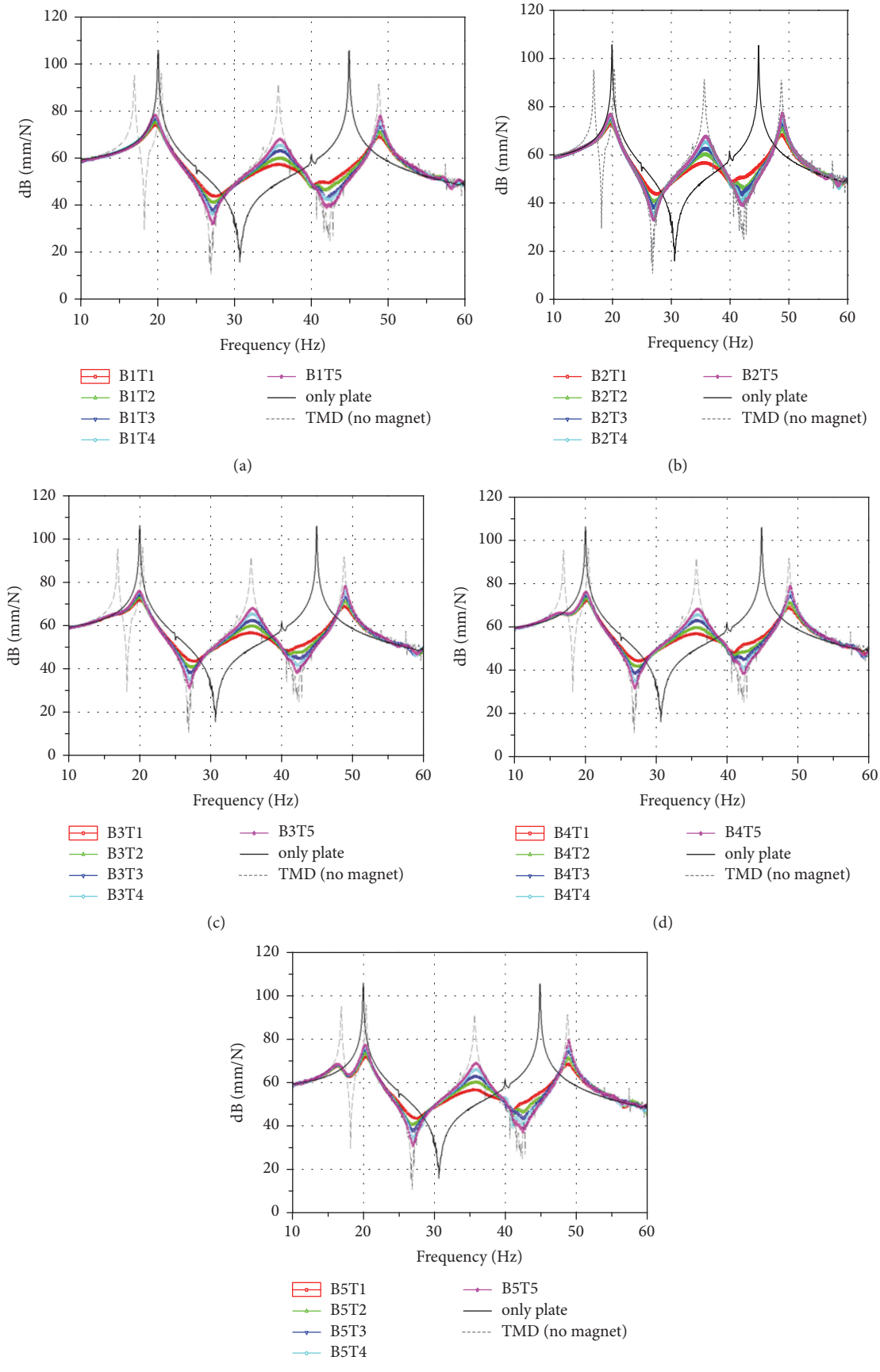

FIGURE 17: FRF results of mTMD with respect to the gap change when $\mu = 0.1$ and $\beta = 0.85$: (a) first TMD gap at 1 mm, (b) first TMD gap at 2 mm, (c) first TMD gap at 3 mm, (d) first TMD gap at 4 mm, and (e) first TMD gap at 5 mm.

Nomenclature

b: Radius of magnet
B: Magnetic flux density
c: Damping coefficient of system
F_o: External force
F_z: Damping force
k: Spring coefficient of system
m: Mass of system
M_0: Magnetization
r_c: Equivalent radius of copper tube
v: Velocity of magnet
β: Natural frequency ratio of system
δ: Thickness of copper
μ: Mass ratio of system
μ_0: Permeability of free space
ς: Damping ratio of system
σ: Conductivity of copper.

Subscripts

b: Base.

Conflicts of Interest

The authors declare that there are no conflicts of interest regarding the publication of this paper.

Acknowledgments

This work was supported by the New & Renewable Energy Core Technology Program of the Korea Institute of Energy Technology Evaluation and Planning (KETEP), a financial resource granted by the Ministry of Trade, Industry & Energy, Republic of Korea (no. 20143030021130). The first and second authors gratefully acknowledge the support in part provided by the Global Surveillance Research Center (GSRC) program funded by the Defense Acquisition Program Administration (DAPA) and Agency for Defense Development (ADD).

References

[1] R. Alkhatib and M. F. Golnaraghi, "Active structural vibration control: a review," *Shock and Vibration*, vol. 35, no. 5, pp. 367–383, 2003.

[2] T. Takagi, J. Tani, S. Matsuda, and S. Kawamura, "Analysis and Experiment of Dynamic Deflection of a Thin Plate with a Coupling Effect," *IEEE Transactions on Magnetics*, vol. 28, no. 2, pp. 1259–1262, 1992.

[3] J. S. Lee, "Dynamic stability of conducting beam-plates in transverse magnetic fields," *Journal of Engineering Mechanics*, vol. 122, no. 2, pp. 89–94, 1996.

[4] D. A. Kienholtz, S. C. Pendleton, and K. E. Richards, "Demonstration of solar array vibration suppression," in *Proceedings of SPIE's Conference on Smart Structures and Materials*, 72, pp. 2193-59, 1994.

[5] G. L. Larose, A. Larsen, and E. Svensson, "Modelling of tuned mass dampers for wind-tunnel tests on a full-bridge aeroelastic model," *Journal of Wind Engineering & Industrial Aerodynamics*, vol. 54-55, no. C, pp. 427–437, 1995.

[6] H. Teshima, Tanaka, K. Miyamoto, K. Nohguchi, and K. Hinata, "Effect of eddy current dampers on the vibrational properties in superconducting levitation using melt-processed YBaCuO bulk superconductors," *Physica C*, vol. 274, pp. 17–23, 1997.

[7] Y. Matsuzaki, D. Ishikubo, T. Kamita, and T. Ikeda, "Vibration control system using electromagnetic forces," *Journal of Intelligent Material Systems and Structures*, vol. 8, no. 9, pp. 751–756, 1997.

[8] Y. Matsuzaki, T. Ikeda, A. Nae, and T. Sasaki, "Electromagnetic forces for a new vibration control system: Experimental verification," *Smart Materials and Structures*, vol. 9, no. 2, pp. 127–131, 2000.

[9] H. A. Sodano and J.-S. Bae, "Eddy current damping in structures," *The Shock and Vibration Digest*, vol. 36, no. 6, pp. 469–478, 2004.

[10] J.-S. Bae, J.-H. Hwang, J.-H. Roh, J.-H. Kim, M.-S. Yi, and J. H. Lim, "Vibration suppression of a cantilever beam using magnetically tuned-mass-damper," *Journal of Sound and Vibration*, vol. 331, no. 26, pp. 5669–5684, 2012.

[11] J.-S. Bae, J.-H. Hwang, J.-H. Roh, and M.-S. Yi, "Development of an electromagnetic shock absorber," *International Journal of Applied Electromagnetics and Mechanics*, vol. 49, no. 1, pp. 157–167, 2015.

[12] M. K. Kwak, M. I. Lee, and S. Heo, "Vibration Suppression Using Eddy Current Damper," *Korean Society for Noise and Vibration Engineering*, vol. 23, pp. 441–453, 2003.

[13] J.-S. Bae, M. K. Kwak, and D. J. Inman, "Vibration suppression of a cantilever beam using eddy current damper," *Journal of Sound and Vibration*, vol. 284, no. 3-5, pp. 805–824, 2005.

[14] H. A. Sodano, J.-S. Bae, D. J. Inman, and W. Keith Belvin, "Concept and model of eddy current damper for vibration suppression of a beam," *Journal of Sound and Vibration*, vol. 288, no. 4-5, pp. 1177–1196, 2005.

[15] H. A. Sodano, J.-S. Bae, D. J. Inman, and W. K. Belvin, "Modeling and application of eddy current damper for suppression of membrane vibrations," *AIAA Journal*, vol. 44, no. 3, pp. 541–549, 2006.

[16] H. A. Sodano, J.-S. Bae, D. J. Inman, and W. K. Belvin, "Improved concept and model of eddy current damper," *Journal of Vibration and Acoustics*, vol. 128, no. 3, pp. 294–302, 2006.

[17] T.-H. Cheng and I.-K. Oh, "A current-flowing electromagnetic shunt damper for multi-mode vibration control of cantilever beams," *Smart Materials and Structures*, vol. 18, no. 9, Article ID 095036, 2009.

[18] T.-H. Cheng and I.-K. Oh, "Vibration suppression of flexible beam using electromagnetic shunt damper," *IEEE Transactions on Magnetics*, vol. 45, no. 6, pp. 2758–2761, 2009.

[19] Z. Wang, Z. Chen, and J. Wang, "Feasibility study of a large-scale tuned mass damper with eddy current damping mechanism," *Earthquake Engineering and Engineering Vibration*, vol. 11, no. 3, pp. 391–401, 2012.

[20] B. Yan, Y. Luo, and X. Zhang, "Structural multimode vibration absorbing with electromagnetic shunt damping," *Journal of Vibration and Control*, vol. 22, no. 6, pp. 1604–1617, 2016.

[21] B. Yan, X. Zhang, and Y. Luo, "Investigation of negative resistance shunt damping for the vibration control of a plate," *International Journal of Applied Electromagnetics and Mechanics*, vol. 45, pp. 93–100, 2014.

[22] S. Xie, P. Li, X. Zhang, and B. Yan, "Vibration suppression of structure with electromagnetic shunt damping absorber," *International Journal of Applied Electromagnetics and Mechanics*, vol. 45, pp. 395–402, 2014.

[23] L. Zihao, L. Wanyou, and Y. Yali, "A study of a beam-like electromagnetic vibration absorber," *Journal of Vibration and Control*, vol. 22, no. 11, pp. 2559–2568, 2014.

[24] J. S. Bae, J. H. Hwang, D. G. Kwag, J. Park, and D. J. Inman, "Vibration suppression of a large beam structure using tuned mass damper and eddy current damping," *Shock & Vibration*, 10 pages, 2014.

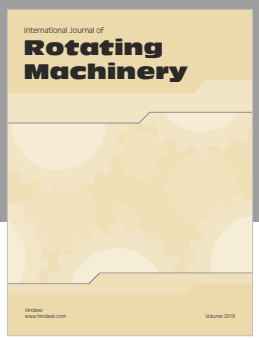

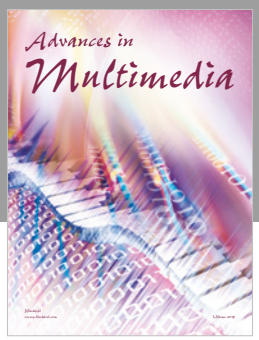

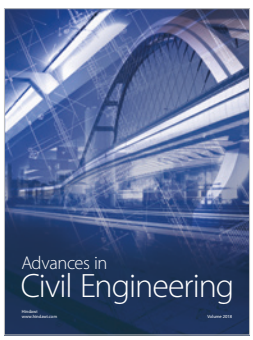

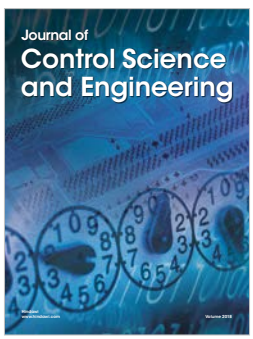

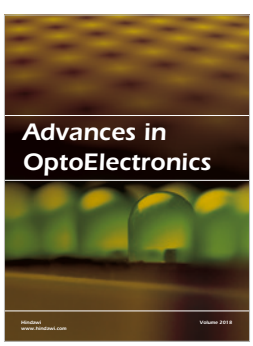

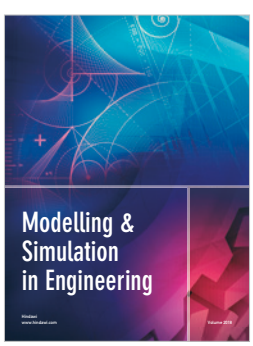

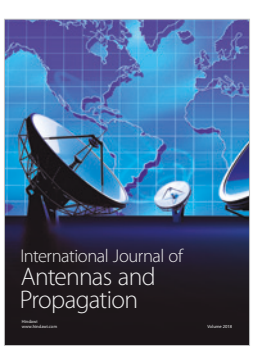

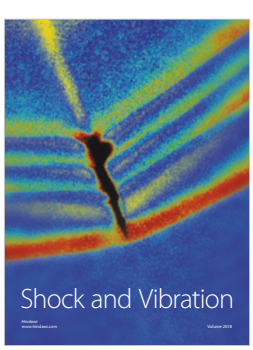

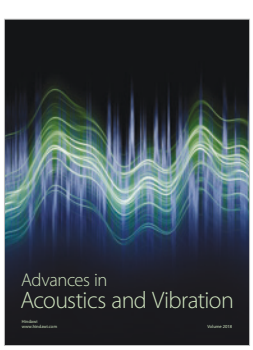

Hindawi

Submit your manuscripts at
www.hindawi.com